Measurements and efficient simulations of bowed bars

Georg Essl[a)]
Computer Science Department, Princeton University, Princeton, New Jersey 08544

Perry R. Cook[b)]
Computer Science Department and Music Department, Princeton University, Princeton, New Jersey 08544

Bowing bar percussion instruments is an increasing part of the repertoire of modern composition and performance. Yet the system has not been studied systematically. In this paper experimental measurements of bars of bar percussion instruments bowed by a double bass bow and by a bowing machine are presented. They examine the relationships between performance parameters and perceptual parameters which are relevant for musical performance. In addition, a new efficient simulation method using a time-domain approach has been developed and the measured results are compared to the simulation. Most measurement results are in good qualitative agreement with the known results of the bowed string. The spectrum of the bowed bar is observed to be harmonic, independent of the harmonicity or inharmonicity of the eigenfrequencies of the bar. Important distinctions from the known results of the bowed string are the weakness or independence of bowing force and velocity on the fundamental frequency and the spectral content of the produced sound. Simulations show qualitative agreement with the measurements. © *2000 Acoustical Society of America.* [S0001-4966(00)03507-4]

INTRODUCTION

Bowed bar percussion instruments have found increasing interest and application in musical composition and performance in recent years. However, the excitation of a sustained oscillation of a bar by means of a rosined bow for musical purposes has not yet been studied systematically.

So far research on bar percussion instruments has focused on the issue of tuning by removing material at various locations along the bar,[1–4] the influence of the resonators on the vibrating bar and the radiated sound,[2,5] and the effect of striking excitation using mallets.[6] Material properties have also been studied.[7,8] Numerical simulations use either finite difference[2,6,5] or finite element methods.[1,4,9] Summaries and reviews of the research on bar percussion instruments are available.[10–12] When the sound of bar percussion instruments is synthesized for real-time performance using electronic sound generation, the above-mentioned finite difference and element methods lack the necessary efficiency on current hardware to be appropriate. Hence, current techniques only model the modes of the system, using modal filters[13,14] or additive sinusoidal synthesis[15,16] ignoring the modal shapes. Hence the notion of physical shape and interaction is lost, and a direct way to use these approaches for bow interactions is not possible. In essence, the spatial dynamics is removed by replacing the actual physical system by an equivalent mass-spring system which models the same modal response. However, the dynamics (in particular the propagation of disturbances) of the original system is lost. Hence it cannot, in general, be expected that nonlinear interactions are captured by the simplified mass-spring model. If the modal shapes are known, the spatial information can be maintained and bow-

ing interactions remain meaningful. This approach has not yet been tried for bars of musical instruments, but was used to study the stick-slip interaction.[17] To use this method, the modal shapes have to be known *a priori.* These are difficult to get analytically because the undercutting of tuned bars make the equations nonlinear and experimental measurement is much more costly than simple frequency analysis.

This paper describes a new simulation method for the purpose of preserving a notion of spatial shape while achieving real-time performance. An *a priori* knowledge of modal shapes is not necessary. A preliminary version of this method and results have been previously published by the authors.[18] It will be described in this paper in more detail and compared to physical experiments in Sec. II.

The action of the bow has only been studied extensively when exciting strings.[19,20] Numerical simulations typically use an efficient time-domain approach which follows from the constant phase delay characteristic of the ideal string equation[21] and this approach has been refined for synthesis purposes.[22,23] The string has also been studied using a finite difference approach.[24–26] The action of the bow on solids is known to be able to excite a sustained oscillation and is especially famous in the creation of Chladni figures.[27] However, a study of the dynamics and kinematics of this system is lacking as is a study of parameters which are relevant for musical performance. The violin bow has also been used to study the excitation of glass harmonica glasses.[28]

The paper is structured in the following way. First, Sec. I contains the description of the measurements. In Sec. I A measurements performed by hand bowing are presented followed by measurements using a bowing machine in Sec. I B. In Sec. II simulations are discussed. In Sec. II A details of the new simulation method are described and in Sec. II B simulation results using this method are presented. Finally in Sec. III we present discussions and conclusions.

[a)]Electronic mail: gessl@cs.princeton.edu
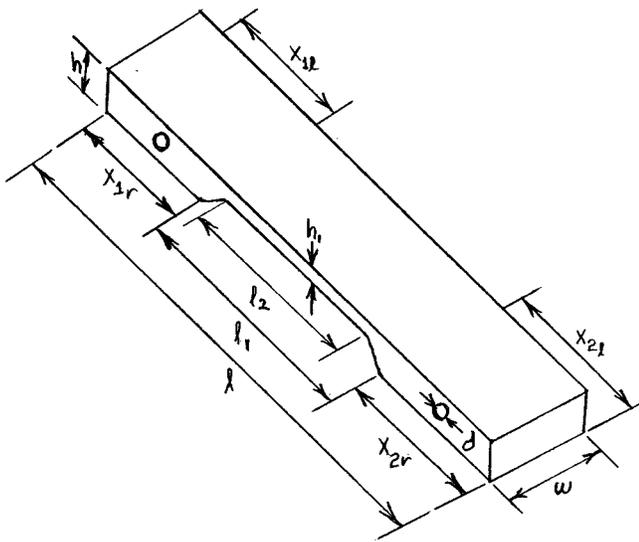[b)]Electronic mail: prc@cs.princeton.edu

FIG. 1. Sketch of shape and dimensions of a bar.

I. MEASUREMENTS

The primary goal of the experiment was the measurement of parameters which are of importance for musical performance when bowing bar percussion instruments. The parameters in control of the performer are primarily bowing velocity and bowing force. Parameters like angle, type of bow, and amount of rosin were not considered in detail in these experiments. The performance parameters of interest were assumed to be loudness, temporal responsiveness, pitch, timbre, and brightness. Other interesting parameters like ease of performance and ''feel'' of the bowing action were not investigated directly. From the measured parameters the region of oscillation is derived, but effects like the ease of locking to higher modes were not considered at all.

Loudness was measured by calculating the energy of the signal. Temporal responsiveness was measured as the time it took from starting the bowing action to reaching a maximum amplitude self-sustained oscillation. This time will be referred to as onset time. Pitch was measured by finding the fundamental in spectra taken from the measured signals. Timbre and brightness was measured by calculating the spectral centroid of the spectra of the measured signals.

Two distinct measurement setups were used. First, a number of bars of different size, shape, and material were bowed by hand using a double bass bow. These measurements were performed to get a qualitative result of most of the described quantities.

In order to get more quantitative and reproducible mea-

surements, a bowing machine was built and one bar was systematically studied for quantitative relationships between input (bow) velocity and force to output amplitude, energy, fundamental frequency, spectral content, and onset time. These results will be described in Sec. I B.

A. Measurements by hand bowing

1. Experimental setup

For hand bowing, two different types of bars were used. One set of bars consisted of bars taken from real musical instruments. These bars are undercut to tune the upper partials to be close to harmonic. In this set, a bar representing the xylophone and marimba family and bars for vibraphones were used. Xylophone and marimba bars are made of wood (typically rosewood) whereas vibraphone bars are metal (typically aluminum).

The second set of bars consisted of wood and aluminum bars of uniform cross section. These have inharmonic partials. The measurement of bars of uniform thickness has two purposes. For one it serves as comparison to the behavior measured for undercut bars. Second, the Euler–Bernoulli equation for constant cross-section and homogeneous material is a linear fourth-order partial differential equation which lends itself to analytical treatment, which is otherwise not easily possible.

A sketch of the typical shape of a bar can be found in Fig. 1. Table I shows the dimensions of the measured bars and Table II shows the position and size of the cord holes. The material constants (Young's modulus and the mass den-

TABLE II. Positions and diameter of cord holes in bars.

	x_{1r} (cm)	x_{1l} (cm)	x_{2r} (cm)	x_{2l} (cm)	d (cm)
Uniform wood	3.9	3.9	3.9	3.9	0.7
$C_4^{\#}$ wood	5.8	5.8	6	5.6	0.5
Uniform aluminum[a]	4	4	4	4	N/A
$F_4^{\#}$ aluminum	5.7	5.8	5.6	6.2	0.6
$F_3^{\#}$ aluminum	7.3	7.4	7.5	6.8	0.6

[a]The aluminum bar had no cord holes. Instead it was held in place by rubber bands on thin plastic rods which were wrapped with felt at the given positions.

TABLE I. Dimensions and material constants of measured bars.

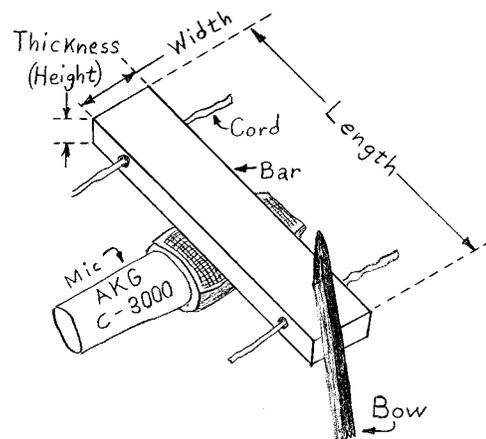|	l (cm)	w (cm)	h (cm)	l_1 (cm)	l_2 (cm)	h_1 (cm)	E (GPa)	ρ (km/m^3)
Uniform wood	38.1	4.05	1.95	N/A	N/A	N/A	10	640
$C_4^{\#}$ wood	30.7	3.5	1.6	17.3	7.0	0.5	16	740
Uniform aluminum	17.8	3.8	0.3	N/A	N/A	N/A	70	2710
$F_4^{\#}$ aluminum	29	3.9	1.8	11.95	5.3	0.6	70	2710
$F_3^{\#}$ aluminum	36.4	5.1	1.8	16.4	9.3	0.5	70	2710

FIG. 2. Experimental setup for hand bowing measurements of bars.

TABLE III. Spectral frequencies of dominant partials of measured bars and theoretical values given as $f_n : f_1$. The left side of the table contains the theoretical prediction for uniform bars and the actually measured ratios of the two measured bars. The right side contains the usual tuning and the measured ratio for tuned bars. The first row contains the actual fundamental frequency f_1 of the bars.

n	Theory	Wooden (uniform)	Aluminum (uniform)	Usual tuning	$C_4^\#$ xylo	$F_3^\#$ vibra	$F_4^\#$ vibra
f_1		693.9	487		280.6	187.3	373.6
2	2.756	2.572	2.756	4	3.932	3.984	3.997
3	5.404	4.644	5.423	10	9.538	10.668	9.469
4	8.933	6.984	8.988		16.688	17.979	15.566
5	13.346	9.723	13.448		24.566	23.679	20.863
6	18.6408		18.680		31.147	33.642	29.440

sity) were taken from a standard reference (see Table 19.1, p. 625 in Ref. 12) and were not measured for the experimental bars.

The bar to be measured was suspended using two stiff cords under tension between two vices. The microphone was placed underneath the middle of the bar. The typical bowing point when bowing xylophone or vibraphone bars in a complete instrument is on the narrow end, as this is the only side which can be conveniently reached with a bow by the performer. Hence our measurements concentrate on bowing positions on the end of the bar. In some bowing strokes, especially when high bowing forces are applied, the oscillation of the mass spring system of the cords and the bar had to be damped by placing one hand on one of the cords and pulling down. The typical setup is depicted in Fig. 2. A rosined double bass bow was used for all measurements.

2. Measurement results

First, the response of the measured bars to impulsive excitation was measured using both a force hammer and a hard plastic glockenspiel mallet. Table III shows the frequencies of the dominant partials of each test bar along with the theoretical values for uniform bars as well as the usual tun-

ing frequencies for undercut bars. As can be seen, the uniform aluminum bar is very close to the values predicted by the Euler–Bernoulli theory. The uniform wooden bar deviates substantially from the theoretical values, for two likely reasons. One is that the bar is not perfectly uniform due to its holes drilled 3.95 cm from both ends with a diameter of 0.75 cm. Second, the thickness is comparable to the width of the bar, in which case the application of the Timoshenko theory is more appropriate, which lowers the frequency of the upper partials.[12]

The bowed bar exhibits a harmonic spectrum, though often weaker partials at the possibly inharmonic eigenfrequencies can be seen. This behavior can also be seen when bowing at positions other than one of the free ends. Bowing at the side is easily possible only with sufficient distance to the suspension holes. When bowing in the middle, the fundamental of the bar can also be excited. For the $F_1^\#$ vibraphone bar bowing in the middle will often lock to the second eigenfrequency of the bar, which lies two octaves above its fundamental eigenfrequency. This tendency to lock to the higher mode can usually only be overcome with increasing friction by tilting the bow or by other means. Another possible way of excitation is to contact the top surface of the bar. By bowing with little bowing force a proper regime of oscillation can be excited.

Using hand bowing, a qualitative relationship between bowing velocity and amplitude as well as between bowing force and amplitude was investigated. It should be noted that constancy of velocity and force within each measurement as well as across measurements (when applicable) were not possible as they are highly dependent on the subjective perception and the skill of the performer. As will be seen in the quantitative measurements using a bowing machine, the lack of constancy of bowing force is likely not a problem as the amplitude appears to be independent of the bowing force.

Figures 3 and 4 show the time domain envelopes of bowing strokes with increasing velocity and increasing force. From the length of the bow and the stroke time, which can be
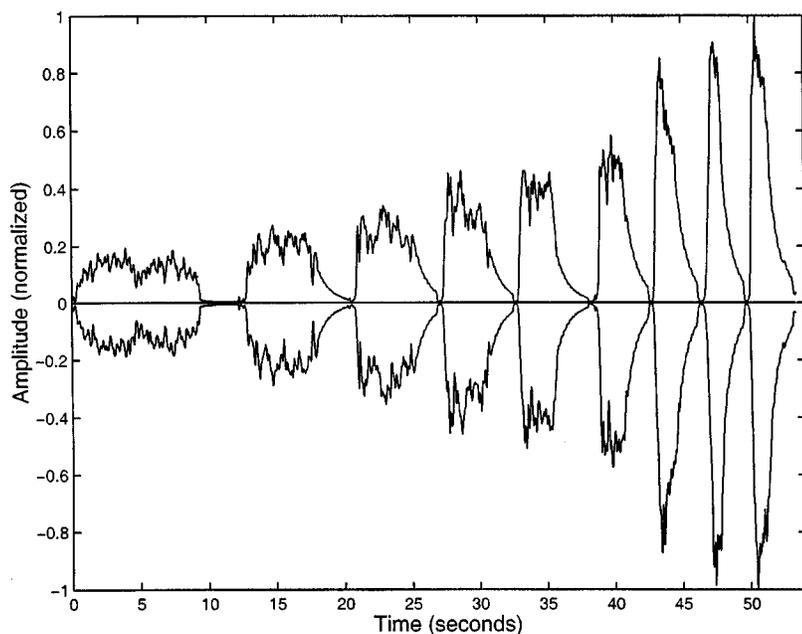

FIG. 3. Time-domain amplitude envelope of hand strokes with increasing velocity and force held approximately constant.
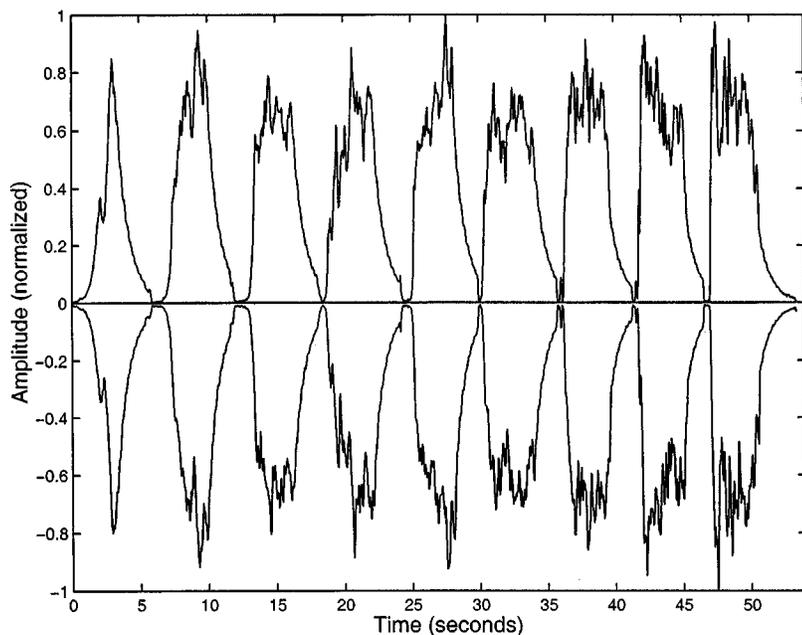
FIG. 4. Time-domain amplitude envelope of hand strokes with increasing force and velocity held approximately constant.

retrieved from the time-domain plot, an average input velocity can be deduced. Setting this velocity in relationship to the amplitude of the signal shows an approximately linear increase of amplitude with increasing velocity. Force was held nearly constant in the velocity measurement. The force measurement shows no clear influence on the amplitude. This finding was later validated by the bowing machine measurements. The time-domain shapes of the force-amplitude relation also hint at a decrease of onset time with increasing force. This result was also quantified using bowing machine measurements, as described in the next section.

B. Measurements using the bowing machine

1. Experimental setup

The $F_3^\#$ aluminum vibraphone bar under investigation (see Table I) was suspended in a rigid bar holder. The holder has two effects. First, it removes the cord modes or other movements which are not of interest while keeping the important degrees of freedom. Second, it allows very high bowing forces to be applied by the bowing machine. As shown in Fig. 5, angled screws were screwed into a wooden base at the positions of the cord holes of the bar. Rubber tips were placed between the metallic holder and the bar to minimize the friction noise and keep a flexible interface. The wooden base was shaped to allow bowing at the narrow side and at the wide side at positions between the suspension holes. In the bowing machine measurement, the bar was pulled towards the bowing machine (which will be described in the next section) by means of a cord which was tied to a hook on one narrow side of the bar holder. When the applied force was measured, the cord was replaced by a spring scale with a scale range of 0 to 2000 g. The microphone position for these measurements was above the middle of the bar as the bar holder did not leave enough space underneath the bar.

2. Bowing machine

The bowing machine consisted of a standard variable speed power drill, a cylindrical drum of hard rubber with a 2.6-cm radius and width of 3.75 cm around which a band of horse hair was wound and glued together at the open ends using super-glue to form a loop. The typical loop width and thickness were comparable to the width of the double bass bow. The horse hair was then rosined. In order to calibrate bowing speed, a bicycle speedometer was added to the drill. The magnet was placed on the rotating part and the pickup sensor was glued to the nonrotating casing of the drill reaching over the magnet. In measurement, the bowing drill was held in place by a vice and the bar was pulled against it. The noise of the drill was damped from the recording by placing
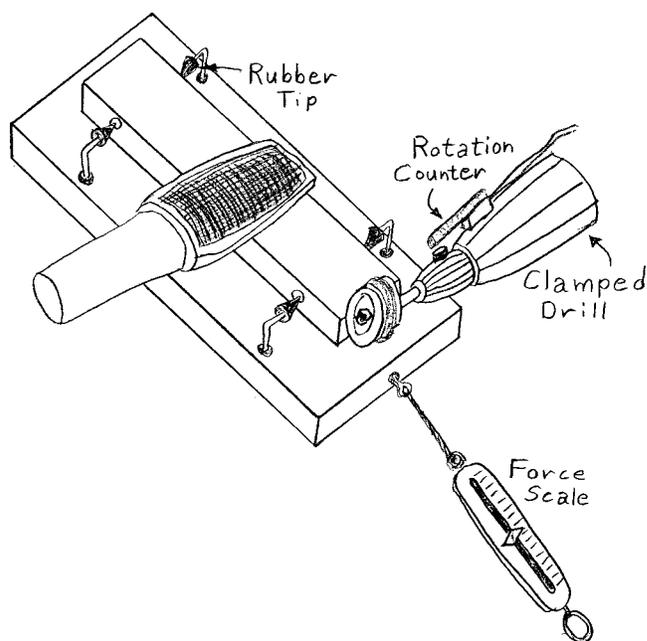

FIG. 5. Experimental setup for bowing machine measurements of bars.

sound-absorbing foam between the drill and the microphone. Also, the microphone position was generally facing away from the drill and towards the primary sound radiation direction of the bar, enhancing the signal-to-noise ratio. The microphone position was adjusted to maximize the signal from the bar while avoiding saturation.

3. Measurement procedure

Two series of measurements were performed using the bowing machine described in the previous section. Before each series the bowing drum had to be rehaired and new rosin was applied. Hence it should be noted that direct quantitative comparisons between these two series are not easily possible. The reason for the need to rehair the bowing machine stems from the fact that the high force measurements at the end of each series resulted in breaking of the hair loop and hence rendered the loop useless for more measurements. There is another reason why the measurements should not be compared between measurement series. The microphone was moved and recalibrated between the series and hence the attenuation of output levels between series should be expected to be different.

The unevenness and change of stiffness of the hair loop at the glue joint yielded an overlap of impulsive excitations over the total bowing excitation. This effect can be expected to influence some of the behavior measured. The impulses overlaying the overall sound were used as an independent measure of velocity because of the occurrence of one impulse per revolution. Later this measurement was correlated with the independent velocity measurement using a speedometer to get an error estimate.

The first series consisted of nine runs starting at a particular bowing speed in gradually increasing forces between 0 and 14 N (or 0 and 2000 g spring scale readings with a relative force contribution of $\sqrt{2}$ due to an angle of 45 degrees). Forces were taken at the following spring scale readings if oscillations occurred: 125, 250, 500, 1000, 1250, 1500, 1750, and 2000 g. In this measurement series, the oscillation was not damped out and restarted at each measurement point, but the force was steadily increased with the bowing machine continuously in contact. The setting of the drill speed was not adjusted, which resulted in a decrease of the actual bowing speed due to the reduced drill speed from the increased force load. All taken measurement points can be seen in Fig. 6. As can be seen, the velocity of each run decreases as a function of input force. The velocity was derived from the recording as described before. The last run (run 9) did not result in oscillation and hence indicates points lying beyond the upper velocity limit.

These measurements were aimed towards finding the regions of oscillation as a function of velocity and force. In addition relative energy as a function of velocity and force was calculated from the recorded sounds and the change in spectral content was characterized using the spectral centroid, which is the center of gravity of the spectrum. The spectral centroid correlates roughly with brightness. Finally, the fundamental frequency of the recorded sounds was also measured. The results will be discussed in subsequent sections.
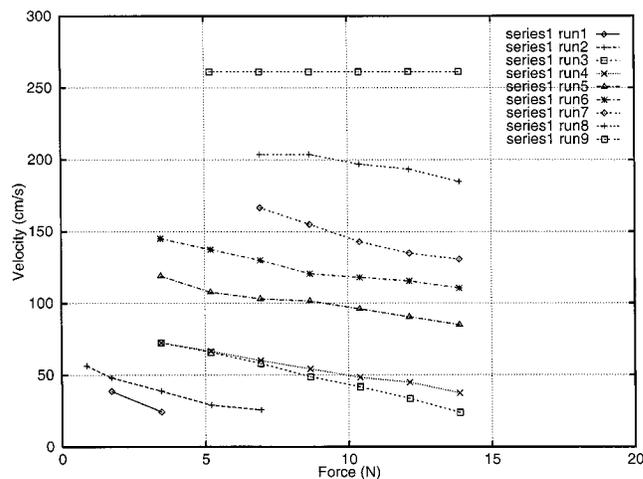

FIG. 6. Bowing machine measurement series 1. Measured input parameters: force and velocity.

The second series consisted of three runs again starting at a particular bowing speed. This time the oscillation was damped out after recording for each measurement point and, using the attached speedometer, the input velocity was adjusted in the attempt to keep the actual bowing speed roughly constant. If a measurement point yielded oscillation, the recording was taken long enough to measure the full oscillation buildup until the maximum and a significant part of the steady state oscillation. Hence, in addition to all the measures derived from series 1, the onset transient time until maximum oscillation was reached was measured in this series. The force range was extended for the first two runs of this series to a maximum force of about 20 N (or a spring scale reading of 2000 g at 0 degree angle).

All measurement points of this series can be found in Fig. 7. The velocities were measured both using the measure of the speedometer and from the recording. A correlation between the two independently measured velocity values shows the average error to be 2.21 cm/s (or 1.2%) with a standard deviation of 2.06 cm/s (or 1.1%). As can be seen, the error is very low. This has to do with the high number of
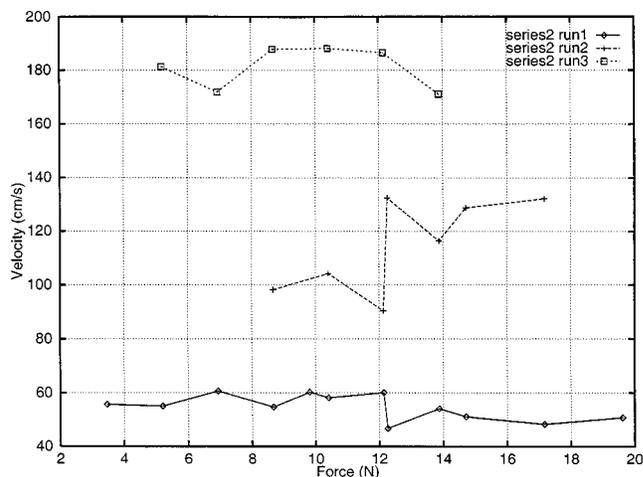

FIG. 7. Bowing machine measurement series 2. Measured input parameters: force and velocity.
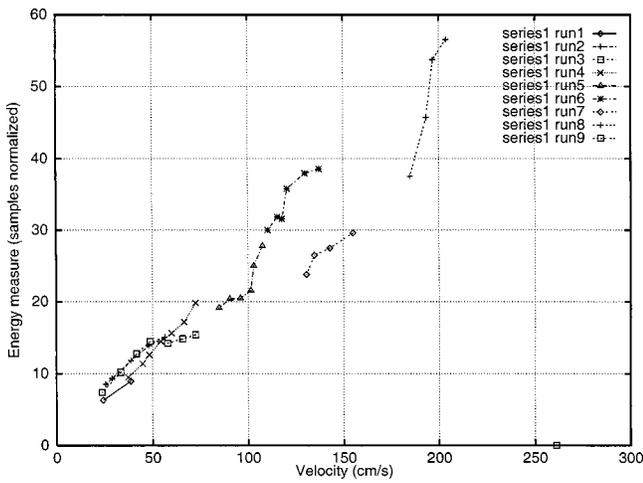
FIG. 8. Bowing machine measurement series 1. Recorded radiation energy as a function of bowing velocity.

revolutions measured in both cases yielding a good resolution.

C. Results of bowing machine measurements

1. Region of oscillation

As can be clearly seen from Fig. 6, the minimum bowing force increases as a function of velocity. A maximum bowing force could only be found for the first two runs of series 1, which are at velocities below 50 cm/s. At higher bowing speeds an upper force limit could not be found within the measurement range. The minimum speed at which steady oscillation was found was 23.83 cm/s with a force of 13.87 N. It should be noted that using the undamped measurement approach of series 1, very low velocities can be achieved even for high forces (as can be seen from run 3 in Fig. 6). (This point is the highest measured force point in this run.) The maximum bowing speed from series 1 is found to be above 203.72 cm/s and below 261.14 cm/s.
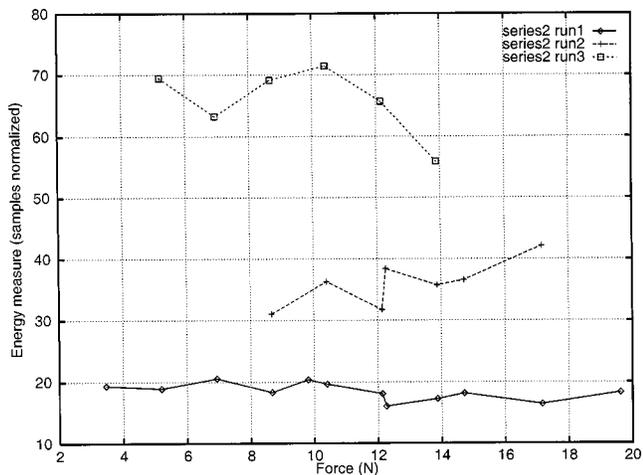

FIG. 9. Bowing machine measurement series 2. Recorded radiation energy as a function of bowing force.
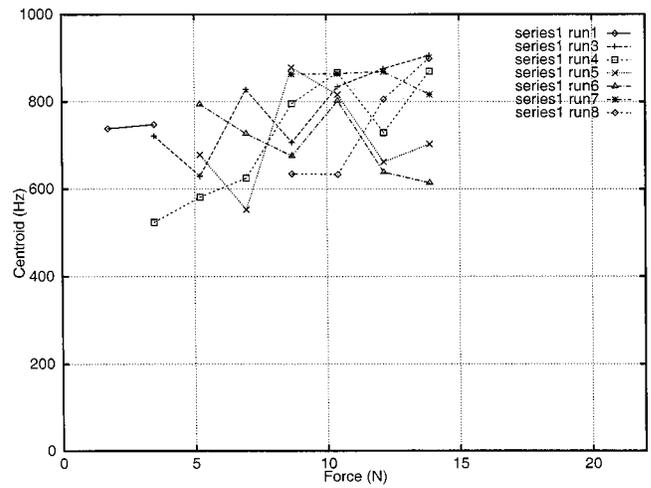

FIG. 10. Bowing machine measurement series 1. Spectral centroid as a function of bowing force. Only measurement points with a clear steady-state oscillation are shown.

2. Energy and power, spectral content, fundamental frequency, and onset times

Both measurement series show that the energy of the fully developed steady state oscillation increases as a function of velocity and the relationship seems to be approximately linear (the measurements of the first series can be seen in Fig. 8). Taking this linear velocity dependency into account, the energy radiation seems to be independent of the input bowing force. (This effect can be seen more clearly in series 2, where the force-energy relationship as depicted in Fig. 9 correlates closely with the force-velocity relationship as depicted in Fig. 7.)

The spectral centroid of series 1 seems uncorrelated with the input force and velocity. No clear upward trend was observed with increasing force (see Fig. 10) in contrast to known behavior of the bowed string. Series 2 verifies this result.

The measurements of the fundamental frequency as a function of velocity and force result in minor fluctuations without a clear trend. In series 1, the mean frequency was 186.67 Hz with a standard deviation of 0.26 Hz (33 data
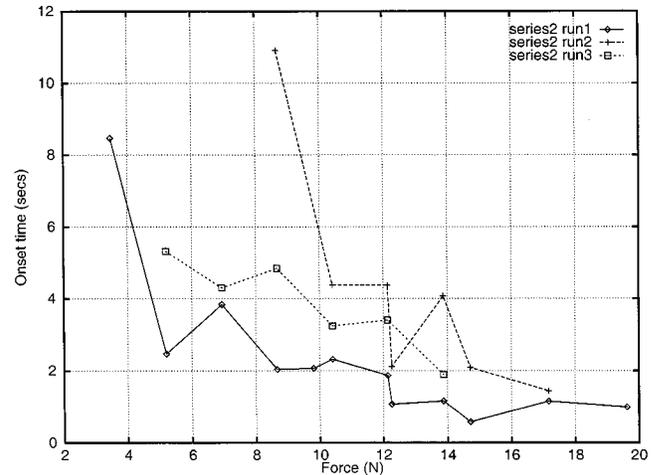

FIG. 11. Bowing machine measurement series 2. Onset time as a function of bowing force.
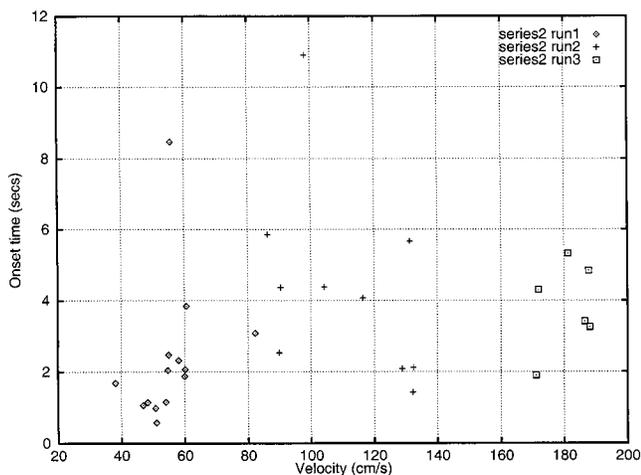
FIG. 12. Bowing machine measurement series 2. Onset time as a function of bowing velocity.

points) and in series 2, the mean frequency was 186.73 Hz with a standard deviation of 0.27 Hz (25 data points). The measurements as a function of velocity seem to indicate a trend towards flattening with increasing velocity, whereas there is no trend observable in dependency of force. In any case, the effect is very small (less than 10 cents) even over the full range. High velocities should be difficult to achieve by hand bowing and hence within the usual bowing domain, the dependency of the fundamental on the bowing parameters is negligible.

Onset time as a function of velocity and force was measured in series 2 only. As was already noted from the time-domain shapes of hand-bowed measurements, there is a clear decrease of the onset times with increasing bowing force (see Fig. 11). The onset time appears uncorrelated with the input bowing velocity (see Fig. 12).

II. SIMULATIONS

A. Simulation method

Taking the finite difference method approach to simulate the model equations can result in remarkably good simulations, but it has the disadvantage of being time consuming to run.[6] The method requires a running time of the order of N calculations, where N is the number of spatial subdivisions. In asymptotic notation this is usually written as $O(N)$. In order to be able to study the qualitative behavior of the system more efficiently and also in order to find a real-time synthesis method for musical performance, a new approach was found. The new method has the advantage of being $O(1)$, that is, independent of the number of spatial sampling points. While modal simulations are also $O(1)$ they either remove the spatial information by ignoring the modal shapes[13–16] or require *a priori* knowledge of the modal shapes.[17] The method to be introduced here will model the spatial information approximately while not requiring the explicit knowledge of modal shapes.

The simulation can be understood in a variety of ways. The derivation presented here is close to the one used to originally derive it. Additional conceptual ways of understanding the methods will be described later.

McIntyre, Schumacher, and Woodhouse's time-domain modeling technique[21] has proven to be very useful in simulating musical instruments with a resonant system which is well approximated by the one-dimensional wave equation. The propagation speed in the resonant part of the instrument (string, pipe) is roughly constant and the computational task involves a convolution with a rather narrow reflection function which contains effects which deviate from the ideal d'Alembert response like weak dispersion due to the weak bending stiffness of the string and dissipation.[29] Smith[22] introduced extensions to the idea taken from scattering filter theory and coined the term *waveguide* for simulations based on this one-dimensional technique.
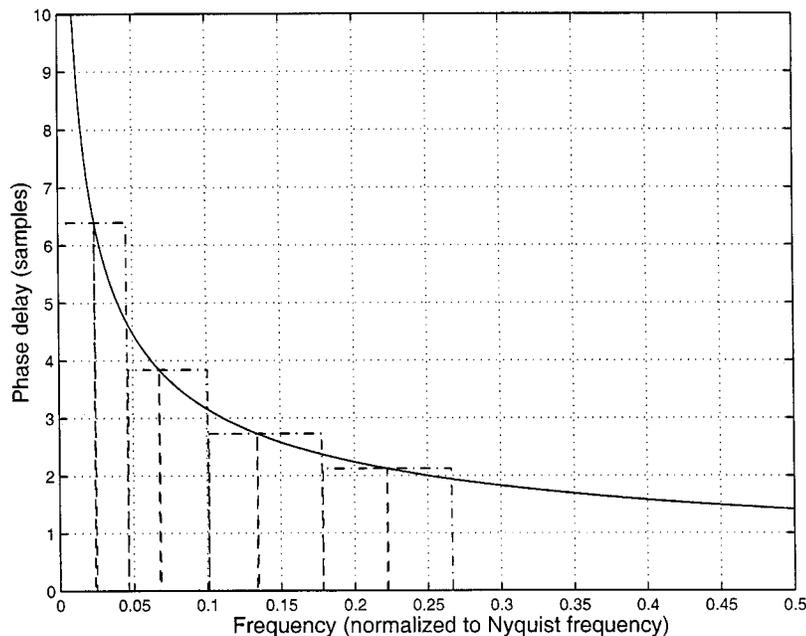

FIG. 13. Discretization of the phase delay in a banded waveguide simulation.

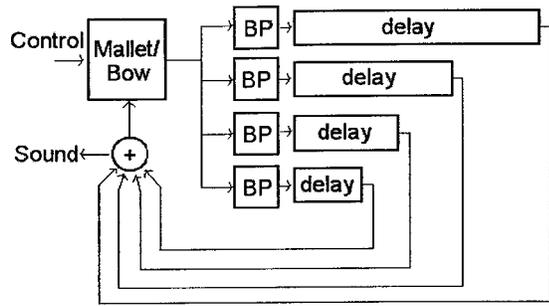G. Essl and P. R. Cook: Simulations of bowed bars

FIG. 14. Flow diagram of the banded waveguide simulation showing excitation and propagation parts.

An attempt to incorporate this idea directly for the Euler–Bernoulli bar equation fails, because the propagation speed is not close to constant but strongly dependent on frequency (see Fig. 13). This makes the direct implementation of the waveguide idea inefficient because the reflection function is not narrow anymore. The nonzero region to be computed by convolution integral becomes large and hence the advantage over implementing a finite difference simulation is removed.

The idea which leads to the banded waveguide simulation is the following. Efficient time-domain simulation is possible if the propagation speed of disturbances in the medium is to a good approximation constant. Instead of trying to implement the propagation speeds at all frequencies correctly, the propagation speeds around the eigenmodes of the systems are modeled correctly and the neighboring frequencies are modeled with the constant propagation speed of the system at the eigenfrequency under consideration. This adds an additional approximation to the system, but it makes the simulation feasible. Another view of this approach is that the wavetrain closures of the system are modeled exactly (within numerical precision) and the approximation gets worse away from the eigenmode. However, the system shows severe damping away from the mode and hence the error is made in the strength of the damping. In the neighborhood of the mode, the error is small. The modal frequencies are modeled accurately to within the numerical resolution.

An illustration of the idea of the approximation is depicted in Fig. 13 assuming the propagation delay of disturbances in a uniform bar, which is a function of the square-root of the frequency in case of the propagating terms in the solution of the Euler–Bernoulli equation for a uniform bar. The assumed constancy of the phase delay within a frequency band can be interpreted as a second quantization of the system in the frequency domain.

In the case of bowing on the narrow side of the bar, disturbances leave only in one direction and only this propagation has to be modeled. The system implemented for simulation can be seen in Fig. 14. As can be seen, this picture follows the general McIntyre, Schumacher, and Woodhouse idea of excitation-resonator decomposition. In the case of a banded waveguide simulation, the resonant part models the propagation of different frequency bands separately.

It should be noted that this approach does not model the spatial shape correctly. There are two ways to illustrate this. First, if only the known propagation speed is modeled, then the near-field oscillations are neglected. Second, if the wavetrain-closure frequencies containing the near-field terms are modeled, then their contribution to the frequency is modeled as propagating waves and not as standing waves.

However, the propagation delay of a physical disturbance is modeled properly. The physical quantity will arrive back at the bowing point after the appropriate time and hence the bow bar interaction is working with reasonable response values.

Another important remark about undercutting should be made. If the undercutting is not too deep, the physics of the bar can be expected to be close to the behavior of the uniform bar and this method is appropriate. The wavetrain closures change with the undercutting and the banded waveguides have to be tuned to the changed frequencies. However, it is important to observe that for severe undercutting, reflections at the points of changing impedance have to
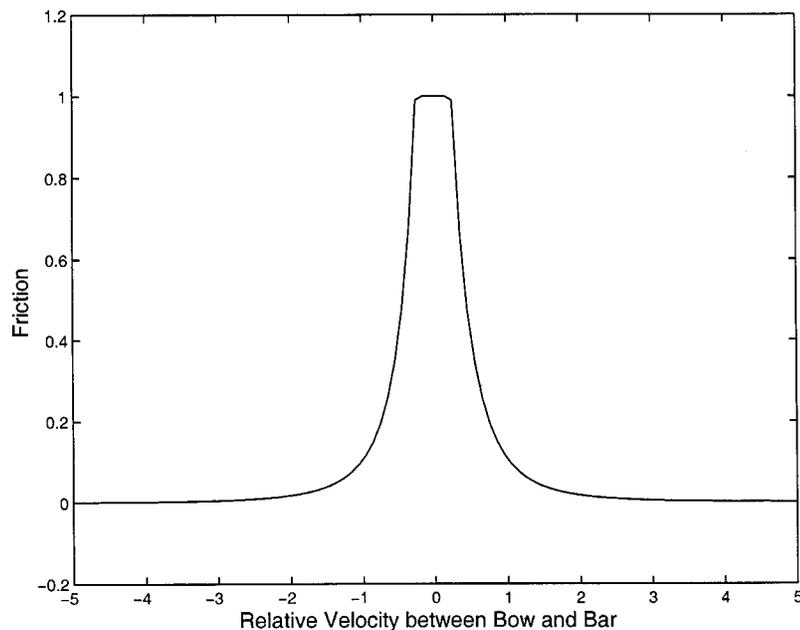

FIG. 15. Friction characteristic used in the banded waveguide simulation. For a relative velocity around zero, the bow exerts a nearly constant strong static friction on the bow whereas when exceeding the relative break-away velocity, the characteristics drops quickly to low dynamic friction.
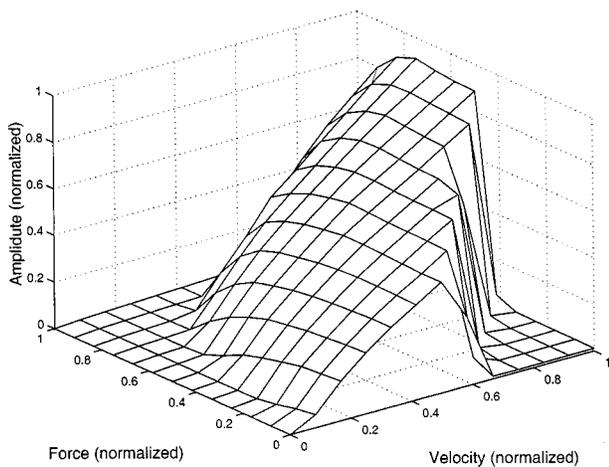
FIG. 16. Amplitude as a function of input force and velocity in a bowed bar simulation using the banded waveguide method.

be expected that are not captured in a straightforward way in an unmodified banded waveguide.

In the implementation used for simulations for this publication, Smith's method of applying the bow nonlinearity to a waveguide simulation[22] was used. This simplified approach simulates the behavior of sticking and sliding friction. During sticking the friction coefficient is independent of the input velocity, but once the differential velocity exceeds a certain value, the friction characteristics drops off rapidly to a weak sliding friction. Figure 15 depicts the actual functional shape used. This model does not contain the hysteresis effect which arises in a slightly more detailed model.[21] Yet the model used seemed to capture the measured phenomena and an extension to incorporate the hysteresis rule has not been found to be necessary. Only the wavetrain closures of the lowest four modes were modeled by banded waveguides. This is reasonable considering the stretching of the partials in a bar. Hence higher modes quickly fall outside the audible range. In addition, higher frequency modes are severely damped. For higher accuracy additional modes could easily be added for low computational cost.

B. Simulation results

Simulations using banded waveguides were performed in 12 steps between normalized input parameters of velocity
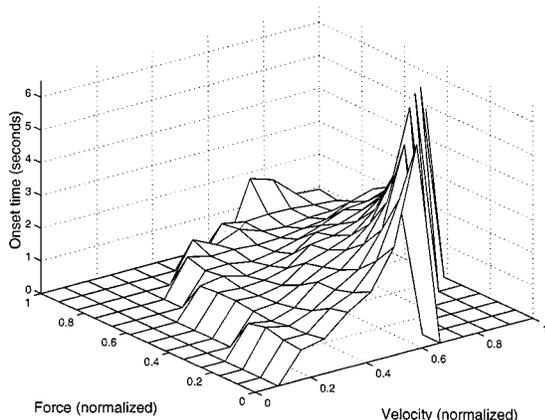

FIG. 17. Onset time as a function of input force in a bowed bar simulation using the banded waveguide method.

and force yielding 144 data points. At each point, the amplitude, onset time, fundamental, and spectral centroid (as measure of spectral content) were extracted from the data.

The simulations show qualitative similarity with the measured parameters. The output amplitude is very nearly linearly dependent on the velocity and largely independent of the force (Fig. 16). A separation of regions of oscillations and nonoscillation can also be seen in this figure. The onset time decreases with increasing force (Fig. 17 is at a normalized input velocity of 0.75). However, the surface plot reveals a more complicated dependency of the onset time with force and velocity which goes beyond the measurements made. Unfortunately, there are too few velocities measured to make a clear comparison of this result with measurement and its interpretation remains open. The fundamental frequency is independent of both force and velocity. The observed spectrum is harmonic. The simulations show that the spectral centroid is independent of both force and velocity, as found in the measurements.

III. CONCLUSIONS

The measurements conducted give evidence that for a set of physical quantities of interest for musical performance, the behavior of the bowed bar is in good qualitative agreement with known behavior of the bowed string while another set of physical quantities shows different behavior. In particular, the increase of output amplitude with increasing velocity and the independence on bowing force is observed in both the bowed string and the bowed bar. Similarly the onset time shows a dependency on the bowing force in both cases. Whereas the simulation of the bar shows also a dependency on bowing velocity as known for the bowed string,[19] this could not be seen from the measurements. The observed modes of the bowed bar are in analogy to the string also harmonic. It should be noted that the action of the bow on solids has often been used to study the modal shape of the solid. However, it seems questionable that the underlying assumption that the oscillation is essentially free and the observed shapes correspond to the eigenmodes of the system. The assumption that the oscillation of the bowed string can be described as a free oscillation has been made early but is known to be flawed.[19] In the case of the bowing of an idealized string, the eigenmodes and the partial frequencies of the nonlinearly excited string coincide, which makes the free oscillation assumption possible and allowed it to yield useful interpretations. As can be seen from the measurements, the eigenmodes of a bar and the partial frequencies of the bowed bar do not coincide and the hope to interpret the system from a free oscillation perspective should be considered inappropriate.

A clear effect of the bowing force and velocity on the fundamental could not be observed in the bar. The same is true for the spectral content. These two parameters show a clear dependency on the input force in the bowed string case. For the bowed string, both effects find intuitive explanation in the interplay between the corner rounding of the string due to stiffness and frequency-dependent dissipation and corner sharpening due to the action of the bow. This intuition does

not lend itself well to the bowed bar, because the kinematics cannot be assumed to be of Helmholtz type.

In the research work on the bowed string, knowing the kinematic motion of the string has led to intuitive explanations for many of the known effects. The vibrational shape of the bowed bar remains unknown and it seems suggestive that knowing the kinematics might help interpret the bowed bar results as well as allowing for a more detailed exploration of the similarities and differences to the bowed string. The authors made an attempt to measure the vibrational shape of the bowed bar using a high-speed CCD camera. Unfortunately the magnification was too weak to yield a clear picture of the vibration. All that could be deduced from the measurements was an upper limit of the maximum mid-point amplitude at medium bowing force at the narrow end of 100 μm which corresponded to a one pixel displacement. This result already has interesting implications on the stick-slip dynamics of bowed bars, because it sets an upper limit to the sticking time at average bowing speed. An average bowing speed of 0.2 m/s yields a maximum sticking time of 500 μs, which is only a short fraction of the total fundamental oscillation of the measured bar, with a fundamental frequency of 186.5 Hz or a period of 5.4 ms. Whereas in the bowed string case the sticking phase is a large part of the oscillatory cycle, this is obviously not the case for the bowed bar.

Simulations using the banded waveguide approach are in qualitative agreement with measurement. Hence the simulation approach seems a reasonable tool for qualitative investigation of the bowed bar phenomenon as well as an attractive efficient simulation method for musical performance.

ACKNOWLEDGMENTS

[1] F. Orduña Bustamante, ''Nonuniform beams with harmonically related overtones for use in percussion instruments,'' J. Acoust. Soc. Am. **90**, 2935–2941 (1991); Erratum: J. Acoust. Soc. Am. **91**, 3582–3583 (1992).

[2] I. Bork, ''Practical tuning of xylophone bars and resonators,'' Appl. Acoust. **46**, 103–127 (1995).

[3] J. Petrolito and K. A. Legge, ''Optimal undercuts for the tuning of percussion beams,'' J. Acoust. Soc. Am. **102**, 2432–2437 (1997).

[4] J. Bretos, C. Santamaría, and J. A. Moral, ''Finite element analysis and experimental measurements of natural eigenmodes and random responses of wooden bars used in musical instruments,'' Appl. Acoust. **56**, 141–156 (1999).

[5] V. Doutaut, D. Matignon, and A. Chaigne, ''Numerical simulations of xylophones. II. Time-domain modeling of the resonator and of the radiated sound pressure,'' J. Acoust. Soc. Am. **104**, 1633–1647 (1998).

[6] A. Chaigne and V. Doutaut, ''Numerical simulations of xylophones. I. Time-domain modeling of the vibrating bars,'' J. Acoust. Soc. Am. **101**, 539–557 (1997).

[7] V. Bucur, *Acoustics of Wood* (CRC, Boca Raton, FL, 1995).

[8] D. Holz, ''Acoustically important properties of xylophone-bar materials: Can tropical woods be replaced by European species?,'' Acust. Acta Acust. **82**, 878–884 (1996).

[9] I. Bork, A. Chaigne, L.-C. Trebuchet, M. Kosfelder, and D. Pillot, ''Comparison between modal analysis and finite element modelling of a marimba Bar,'' Acust. Acta Acust. **85**, 258–266 (1999).

[10] J. L. Moore, ''Acoustics of Bar Percussion Instruments,'' Ph.D. thesis, Ohio State University, Columbus, 1970.

[11] T. D. Rossing, ''Acoustics of percussion instruments—Part I,'' Phys. Teach. **14**, 546–556 (1976).

[12] N. H. Fletcher and T. D. Rossing, *The Physics of Musical Instruments*, 2nd ed. (Springer Verlag, New York, 1998).

[13] J. Wawrzynek, ''VLSI Models for Sound Synthesis,'' in *Current Directions in Computer Music Research*, edited by M. Mathews and J. Pierce (MIT, Cambridge, 1989), Chap. 10, pp. 113–148.

[14] P. R. Cook, ''Physically informed sonic modeling (PhISM): Synthesis of percussive sounds,'' Comput. Music J. **21**, 38–49 (1997).

[15] X. Serra, ''A Computer Model for Bar Percussion Instruments,'' in *Proceedings of the International Computer Music Conference (ICMC)* (International Computer Music Association (ICMA), The Hague, 1986), pp. 257–262.

[16] K. van den Doel and D. Pai, ''The Sound of Physical Shapes,'' Tech. Rep., Dept. of Computer Science, University of British Columbia, Canada, Vancouver (1996).

[17] J. H. Smith, ''Stick-Slip Vibration and its Constitutive Laws,'' Ph.D. thesis, University of Cambridge, March 1990.

[18] G. Essl and P. R. Cook, ''Banded Waveguides: Towards Physical Modeling of Bowed Bar Percussion Instruments,'' in *Proceedings of the International Computer Music Conference (ICMC)* (International Computer Music Association (ICMA), Beijing, China, 1999), pp. 321–324.

[19] L. Cremer, *The Physics of the Violin* (MIT, Cambridge, 1984).

[20] C. Hutchins and V. Benade, eds., *Research Papers in Violin Acoustics 1975–1993* (Acoustical Society of America, Woodbury, NY, 1997).

[21] M. E. McIntyre, R. T. Schumacher, and J. Woodhouse, ''On the oscillation of musical instruments,'' J. Acoust. Soc. Am. **74**, 1325–1344 (1983).

[22] J. O. Smith, ''Efficient Simulation of the Reed-Bore and Bow-String Mechanisms,'' in *Proceedings of the International Computer Music Conference (ICMC)* (International Computer Music Association (ICMA), The Hague, 1986), pp. 275–280.

[23] S. Serafin, C. Vergez, and X. Rodet, ''Friction and Application to Real-time Physical Modeling of a Violin,'' in *Proceedings of the International Computer Music Conference (ICMC)* (International Computer Music Association (ICMA), Beijing, China, 1999), pp. 216–219.

[24] A. Chaigne and A. Askenfelt, ''Numerical simulations of piano strings. I. A physical model for a struck string using finite difference methods,'' J. Acoust. Soc. Am. **95**, 1112–1118 (1994).

[25] A. Chaigne and A. Askenfelt, ''Numerical simulations of piano strings. II. Comparisons with measurements and systematic exploration of some hammer-string parameters,'' J. Acoust. Soc. Am. **95**, 1631–1640 (1994).

[26] M. Palumbi and L. Seno, ''Physical modeling by directly solving wave PDE,'' in *Proceedings of the International Computer Music Conference (ICMC)* (International Computer Music Association (ICMA), Beijing, China, 1999), pp. 325–328.

[27] M. D. Waller, *Chladni Figures—A Study in Symmetry* (Bell, London, 1961).

[28] T. D. Rossing, ''Acoustics of the glass harmonica,'' J. Acoust. Soc. Am. **95**, 1106–1111 (1994).

[29] J. Woodhouse, ''On the playability of violins. Part I: Reflection functions,'' Acustica **78**, 125–136 (1993).